Limited data prevent assessment of role of climate change in deadly floods affecting highly vulnerable communities around Lake Kivu

Authors

1. Joyce Kimutai, *Grantham Institute, Imperial College London, UK*
2. Dieudonne Nsadisa Faka, *The Organisation of African, Caribbean and Pacific States, Brussels, Belgium*
3. Prosper Ayabagabo, *Rwanda Meteorology Agency, Kigali, Rwanda*
4. Clair Barnes, *Grantham Institute, Imperial College London, UK*
5. Mariam Zachariah, *Grantham Institute, Imperial College, London, UK*
6. Izidine Pinto, *Royal Netherlands Meteorological Institute (KNMI), De Bilt, The Netherlands*
7. Gerbrand Koren*, Copernicus Institute of Sustainable Development, Utrecht University, Utrecht, the Netherlands*
8. Maja Vahlberg, *Red Cross Red Crescent Climate Centre, The Hague, the Netherlands*
9. Roop Singh, *Red Cross Red Crescent Climate Centre, The Hague, the Netherlands*
10. Dorothy Heinrich, *Red Cross Red Crescent Climate Centre, The Hague, the Netherlands*
11. Emmanuel Raju, *Department of Public Health, Global Health Section & Copenhagen Centre for Disaster Research, University of Copenhagen, Denmark*
12. Lisa Thalheimer, *United Nations University, Institute for Environment and Human Security, Bonn, Germany*
13. Sajanika Sivanu, *Red Cross Red Crescent Climate Centre, The Hague, the Netherlands*
14. Friederike Otto, *Grantham Institute, Imperial College London, UK*

Reviewers

Sjoukje Philip, *Royal Netherlands Meteorological Institute (KNMI), De Bilt, The Netherlands*
Guigma Kiswendsida, *Red Cross Red Crescent Climate Centre, The Hague, the Netherlands*
Leonard Nioulé, *International Federation of Red Cross and Red Crescent Societies, Goma, North Kivu, Democratic Republic of Congo*

Main findings

- We urgently need robust climate data and research in this highly vulnerable region. The scarcity and inaccessibility of meteorological data, as well as inadequate performance of climate models meant we couldn't confidently evaluate the role of climate change in the rainfall that led to flooding. This limitation applies also to information on the impact, vulnerability, and exposure of people to heavy rainfall, a critical gap that has been highlighted by numerous studies.
- The death toll and destruction from the floods in South Kivu, DRC and western Rwanda was extreme, and reflects the high vulnerability and exposure of people to flooding in this region.

- The history of conflict in the region and instability has contributed to underdevelopment and a lack of basic services and infrastructure. The combination of protracted conflict, displacement, under-development, poverty and land degradation, creates a recipe for disaster when an extreme weather event strikes, making it more difficult for people to cope and bounce back from the disaster.
- The conflict and violent clashes between state and non-state groups have led to large-scale displacement in South Kivu, DRC and western Rwanda in 2023, with displaced populations being more susceptible to flood and landslide impacts due to their living conditions (e.g. temporary shelters) and precarious situation. The floods further displaced thousands of people, destroyed water, sanitation and hygiene infrastructure, damaged agricultural fields leading to increased risk of food insecurity, waterborne illnesses and protection issues after the initial recovery phase ends.
- Deforestation in order to clear land for settlements, agriculture, and mining, has resulted in widespread soil erosion around Lake Kivu, contributing to an increasing risk of landslides. A lack of capacity of the government to enforce limits or regulation on land degrading practices.
- While the DRC's mineral reserves are critical for global manufacturing and the transition to a low carbon economy and its forests act as a key carbon sink for the world's carbon polluters, the country continues to suffer from the impacts of extreme weather which are amplified by mining activities that contribute to land and water degradation, labour abuses, and conflict.
- We examined three different combinations of spatial and temporal extent to look at heavy rainfall events in the region of the floods to see whether there are trends in either of these in the different available data products. In different datasets there are trends in seasonal and short term heavy rain in both directions (increases and decreases), as well as data showing no trend.
- Climate models show no significant trends in heavy precipitation over the region since the preindustrial climate, but an increase in short term heavy rainfall for a 0.8C warmer world (2C global warming). However, this is no indication that there is no trend, as the uncertainty is very high.
- The increase in heavy precipitation with future warming is in line with projections from the IPCC over the whole of central and eastern Africa, which also show an increase in heavy rainfall.
- While the scarcity of data does not allow us to draw any conclusions on the role of climate change in the floods today, the potential for a further increase in heavy rainfall in this flood and landslide prone area highlights an urgent need to reduce vulnerability
- Better observations, improved access to meteorological data and more research are urgently needed in the region to improve early warning systems.

1 Introduction

At the beginning of May 2023, severe flooding around Lake Kivu devastated communities in Rwanda and the Democratic Republic of Congo (DRC). Flooding and landslides led to at least 595 fatalities with 460 reported deaths in the DRC (TimesLive, 25 May 2023; Xinhua, 12 May 2023) and 135 in Rwanda (The East African, 7 May 2023; Monitor, 7 May 2023). The flooding and landslides

reportedly occurred after heavy rainfall as early as mid April and thereafter during the first few days in May, particularly on 2-4 and 8 May 2023 (Floodlist, 5 May 2023). The daily rainfall record in Rwanda was broken on the 2nd of May 2023 with 182.6 mm of rainfall at Mushubati station in the Rutsiro District (Meteo Rwanda, 6 May 2023). This event was characterised by severe flooding of the Sebeya river in the Rubavu district, flash floods, landslides and unsustained house collapses in the affected regions (Reliefweb 15 May 2023; 15 June 2023). Western Rwanda is situated on the steep mountains that separate the Congo and the Nile Basin. Major flooding occurred following heavy rains from 8pm on Tuesday May 2 to 9am on May 3 over Rutsiro, Rubavu, Karongi, Ngororero and Musanze districts of Rwanda and from 6pm on Thursday May 4 to 8pm on May 05, 2023 over Kalehe territory in the province of South Kivu, in the DRC (Floodlist, 8 May 2023). This event caused several human fatalities, and damages to property were recorded after the Chabondo river broke its banks flooding Nyamukubi, village of Bushushu, Mbinga-south group in the Buhavu chiefdom, and the Kalehe/sud-Kivu territory to the east of the DRC. The river floods caused major landslides carrying public infrastructure and homes. Electricity and drinking water supplies were disrupted. Around 142 bodies were discovered in Bushushu, 132 in Nyamukubi and 120 floating corpses were found on Lake Kivu around Idjwi Island (Agenzianova, 7 May 2023). Families were left stranded waiting for help and sought temporary shelter in straw huts. As a result, the risk of water-borne disease outbreaks went high.

Lake Kivu is one of seven African Great Lakes, located between Rwanda and DRC (Figure 1). The region experiences two main rainy seasons: from September to December (hereafter, SOND) and from March to May (hereafter, MAM). However the spatial and temporal variations of rainfall in this region are large due to the topographic heterogeneity and presence of large water bodies (Meteo Rwanda). Observations around and on Lake Kivu from 2013 to 2016 indicate moderate to high rainfall also occurs outside the main rainy seasons (Rooney et al., 2018). Flooding and in particular landslides are the most common hydrometeorological disasters in both the DRC side and Rwandan side of Lake Kivu (Maki Mateso et al., 2023). The lake region is densely populated with 160 inhabitants per square kilometre, the majority of whom are dependent on rain-fed agriculture and thus highly vulnerable to extreme weather (Bagalwa et al., 2021).

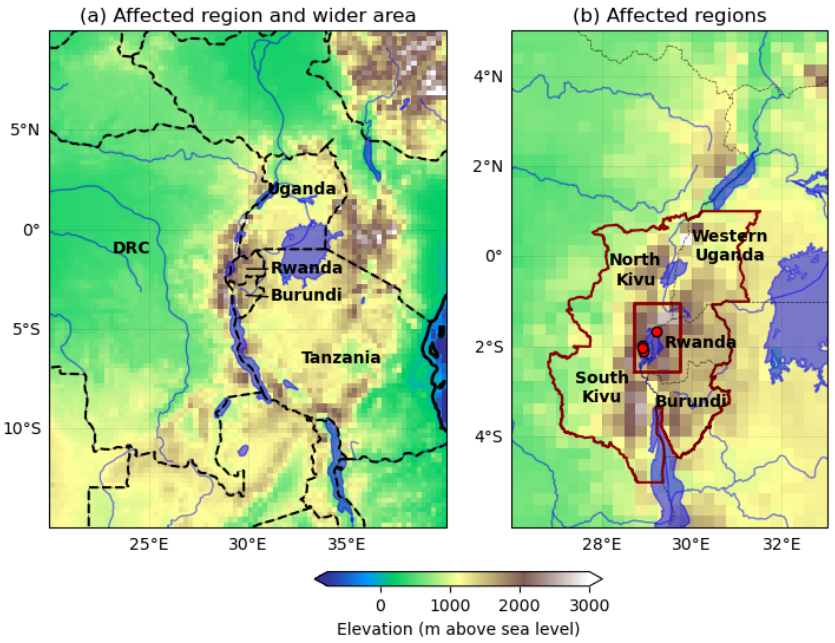

Figure 1: Physical geography of the (a) the affected region of East Africa and (b) the smaller region around Lake Kivu, bounded by the rectangle in (a), in which the most severe flooding occurred. The irregular red boundary in (b) denotes the mountainous region in which severe flooding was reported, and the smaller rectangle denotes the Lake Kivu region in which impacts were felt on May 2nd. The red dots indicate the villages where flooding was particularly severe: Kalehe, Nyamukubi, Goma, and Bushushu.

1.1 Climatological context

Generally in the tropics, convective rainfall events are characterised by increasing instability and moisture content due to strong low-level large-scale convergence, vertical velocity and lifting (Nicholson, 2022; Breugem et al.,2020). In East Africa, the high seasonal and interannual variability of rainfall in the MAM season is a result of the complex interaction between local factors, regional circulation patterns and remote forcings/teleconnections (Nicholson, 2017;Cook & Vizy, 2013;Rowell et al., 2015). Large-scale and localised convergence zones can result from low-level airflows from different directions, canalisation or reinforcement of small-scale flows, and sea breezes. The contrasted topographical settings can induce widespread dynamic effects through mesoscale circulation systems. Lifting mechanisms and convective instability are influenced by land surface characteristics and mountains. Therefore rainfall is mainly driven by zonal wind anomalies, advection of moisture and zonal propagation of convection (Camberlin and Wairoto, 1997; Okoola, 1999; Camberlin & Okoola, 2003;Pohl & Camberlin, 2006a;Hastenrath et al., 2010;Pohl & Camberlin, 2011;Omondi et al., 2012;Hogan et al., 2015;Vigaud et al., 2016; Nicholson, 2017; Vellinga & Milton, 2018). The three main moisture sources for rainfall in the region are Lake Victoria, the Indian Ocean, and the humid layer of the Congo airmass (e.g. Ngarukiyimana 2017).

As one of the three core regions of convection in the global tropics, the Congo Basin plays a significant role in planetary circulation and the Earth system through the control of weather patterns and atmospheric dynamics in the region. The region also stands as a vulnerable hotspot for climatic change, magnifying concerns about the local responses to global warming (Creese et al., 2019). This region is experiencing recurrent floods and droughts and it is likely that climate change will worsen these events (Karam et al., 2022). Future changes to the Congo Basin climate system are bound to have regional and tropics-wide implications. Given its criticality, precise monitoring of the climate in equatorial Africa assumes an imperative role in understanding and addressing the challenges posed by the Congo Basin's impact on our planet's climate system. Assessing the trend in the number of rainy days and mean rainfall over Rwanda, Muhire and Ahmed, (2015) found that areas located in the highlands and around Kivu Lake are becoming wetter compared to the rest of the country. The highlands are consequently experiencing more extreme rainfall events, with the eastern lowlands and the central plateau becoming drier. Literature on observed changes in heavy precipitation is very limited over central and southern East Africa, with even global studies noting insufficient data to assess trends (Dunn et al., 2020). This scarcity of ground datasets is due to a reduction in the number of weather stations in the region (e.g., Climate Hazards Center). For instance, on the DRC side, the initial network of meteorological observations was formed, at the accession of the country to independence, from 125 mixed-use stations: synoptic and climatological. Over time, due to the various event conflicts and the non-renewal of instruments the number of operational stations nationwide has reduced to 28, mostly located at the national airport with relatively heavy traffic (MEDD, 2015). The lack of measurement stations affects the quality of precipitation estimates over the region (Awange et al., 2015; Tarek et al. 2021), further complicating the analysis of precipitation extremes. At higher warming level projections, GCMs show an increase in heavy precipitation in these regions (Seneviratne et al., 2021).

1.2 Event Definition

In order to understand the trends in the short-term precipitation related to the severe flooding at the beginning of May, we look at two event definitions - (i) RX1day, the maximum during each MAM rainy season of 1-day precipitation over the region encompassing Lake Kivu (the small rectangular domain in Figure 1); and (ii) RX5day, the maximum during MAM of the 5-day accumulated precipitation over the irregularly shaped region outlined in red in Figure 1. In addition, to understand whether the preceding months have been particularly wet, potentially saturating the soil and exacerbating the severity of the floods, we also consider a third event definition: (iii) the accumulated MAM precipitation over this same irregularly-shaped region. The smaller of these regions (hereafter, the Lake Kivu region) captures only the region around Lake Kivu where the most severe impacts were felt (Figure 2), while the larger region (hereafter, the DRC/Rwanda region) captures a wider mountainous region in which severe impacts were experienced, including Rwanda, Burundi, the North and South Kivu provinces of DRC, and part of western Uganda (Figure 3).

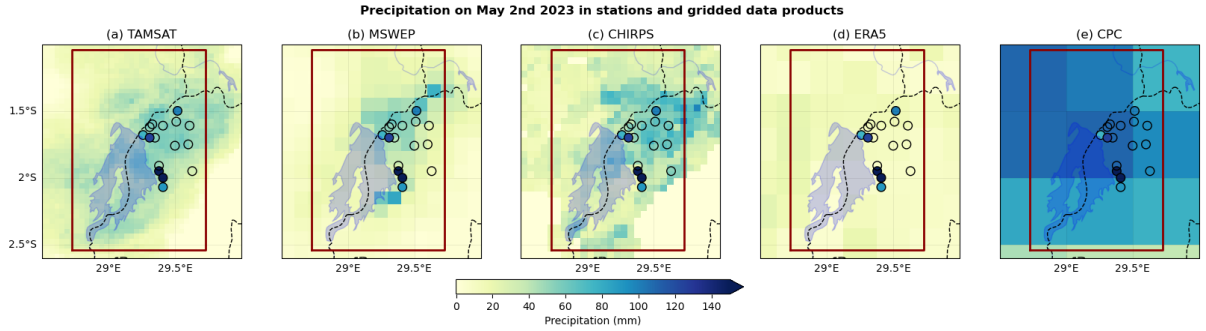

Figure 2: Precipitation on May 2nd 2023 over the Lake Kivu region in five gridded data products: (a) TAMSAT, (b) MSWEP, (c) CHIRPS, (d) ERA5, (e) CPC. The irregularly-shaped blue shaded region is Lake Kivu, and the red border indicates the small region around Lake Kivu for which RX1day was computed. Filled circles represent six stations (Gihango, Mushubati, Nyundo, Shingiro, Gisenyi Aero and Rubungera Met) where observations of precipitation on this day were available, with the shading reflecting the same colour scale as used in the maps. In four of these stations (Gihango, Mushubati, Nyundo, Shingiro) a new daily precipitation record was set on this day. Empty circles represent stations where data was used for validation of the gridded data products, but where data was unavailable for May 2nd 2023.

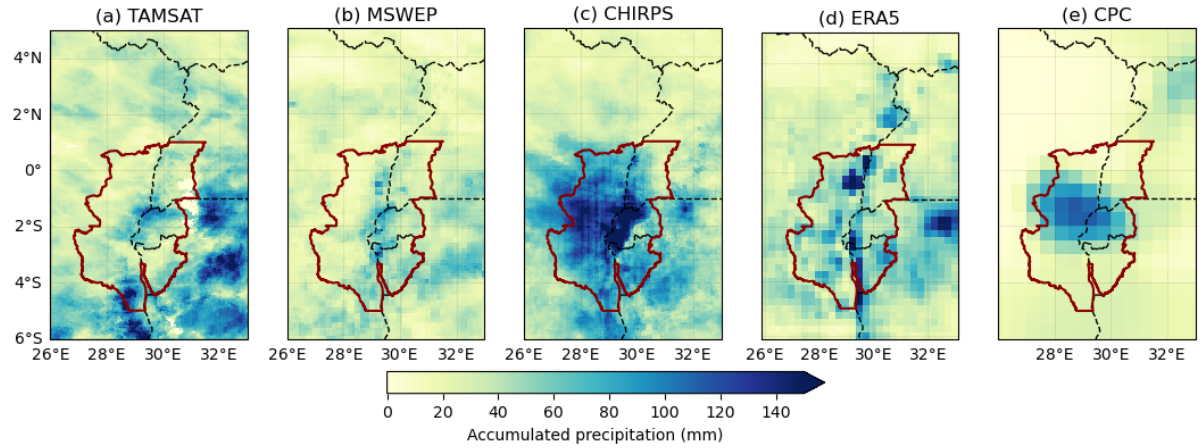

Figure 3: 5-day accumulated precipitation in gridded data products from May 1st-5th 2023 over the region surrounding Lake Kivu: (a) TAMSAT, (b) MSWEP, (c) CHIRPS, (d) ERA5, (e) CPC. The red border indicates the larger region around Lake Kivu for which RX5day was computed.

2 Data and methods

2.1 Observational data

Five gridded observational data products were analysed to estimate the amount of precipitation in the affected region.

1. TAMSAT: Rainfall product based on high-resolution Meteosat thermal infrared (TIR) imagery, calibrated using rain gauge observations (Maidment et al., 2014, 2017; Tarnavsky, 2014). Daily data are available at approximately 4 km spatial resolution across the whole of Africa. The data product is developed by the Tropical Applications of Meteorology using

SATellite data and ground-based observations (TAMSAT) group at the University of Reading, UK.

2. CHIRPS: Observational daily dataset developed by the UC Santa Barbara Climate Hazards Group (Climate Hazards Group InfraRed Precipitation with Station data; Funk et al., 2015b). Daily data are available at 0.05° resolution for East Africa, from 1981-present. The product incorporates satellite imagery with in-situ station data.

3. MSWEP: The Multi-Source Weighted-Ensemble Precipitation (MSWEP) v2.8 dataset (updated from Beck et al., 2019) is fully global, available at 3-hourly intervals and at 0.1° spatial resolution, available from 1979 to ~3 hours from real-time. This product combines gauge-, satellite-, and reanalysis-based data for reliable precipitation estimates.

4. ERA5: A reanalysis product, available at 0.25° spatial resolution globally from 1950 onwards. Variables from ERA5 are not directly assimilated from observations, but are generated by atmospheric components of the European Centre for Medium-Range Weather Forecasts' Integrated Forecasting System (Hersbach et al., 2020).

5. CPC: The gridded product from NOAA PSL, Boulder, Colorado, USA known as the CPC Global Unified Daily Gridded data, is available at 0.5° x 0.5° resolution, for the period 1979-present. Data are available from NOAA.

Direct observations of daily precipitation from the stations in Rwanda shown in Figure 2 were provided by Rwanda Meteorology Agency (MeteoRwanda). These data only span the years from 1980-2021, so can only be used to evaluate the historic performance of the gridded data products, rather than during the period of interest. These data were supplemented with observations of record-breaking precipitation during 2023 from the Agency's portal. Four stations (Gihango, Mushubati, Nyundo and Shingiro; darker shaded dots in Figure 2) were found to have experienced record-breaking precipitation on May 2nd. Historical station data was also provided by the DRC's meteorological agency but did not span May 2023; data for other regions were not available.

As a measure of anthropogenic climate change we use the (low-pass filtered) global mean surface temperature (GMST), where GMST is taken from the National Aeronautics and Space Administration (NASA) Goddard Institute for Space Science (GISS) surface temperature analysis (GISTEMP, Hansen et al., 2010 and Lenssen et al. 2019).

2.2 Model and experiment descriptions

We use two multi-model ensembles from climate modelling experiments using very different framings (Philip et al., 2020): regional climate models and Sea Surface temperature (SST) driven global circulation high resolution models.

1. Coordinated Regional Climate Downscaling Experiment CORDEX-CORE (0.22° resolution, AFR-22) multi-model ensemble (Gutowski et al., 2016; Giorgi et al., 2021), consisting of 9

simulations produced by combinations of 3 Global Climate Models (GCMs: HadGEM2-ES, MPI-ESM-LR and NorESM1-M) and 3 Regional Climate Models (RCMs: CCLM5-O-15, RegCM4-7 and REMO2015). These simulations are composed of historical simulations up to 2005, and extended to the year 2100 using the RCP8.5 scenario.

2. HighResMIP SST-forced model ensemble (Haarsma et al. 2016), the simulations for which span from 1950 to 2050. The SST and sea ice forcings for the period 1950-2014 are obtained from the 0.25° x 0.25° Hadley Centre Global Sea Ice and Sea Surface Temperature dataset that have undergone area-weighted regridding to match the climate model resolution. For the 'future' time period (2015-2050), SST/sea-ice data are derived from RCP8.5 (CMIP5) data, and combined with greenhouse gas forcings from SSP5-8.5 (CMIP6) simulations (see Section 3.3 of Haarsma et al. 2016 for further details).

2.3 Statistical methods

In this analysis we analyse time series of (i) RX1day in the MAM season over the Lake Kivu region, (ii) RX5day in MAM over the DRC/Rwanda region and (iii) Average rainfall during MAM over the DRC/Rwanda region, using the longest available records of observed and reanalysis data. Methods for observational and model analysis and for model evaluation and synthesis are used according to the World Weather Attribution Protocol, described in Philip et al. (2020), with supporting details found in van Oldenborgh et al. (2021), Ciavarella et al. (2021) and here.

The analysis steps in the protocol include: (i) trend calculation from observations; (ii) model validation; (iii) multi-method multi-model attribution and (iv) synthesis of the attribution statement. To statistically model the event under study, we use a nonstationary GEV distribution for the seasonal maxima (RX1day and RX5day) and a nonstationary Gaussian distribution for the MAM seasonal average rainfall. In all of these models, the location parameter shifts with the GMST, while the dispersion (the ratio of the standard deviation to the mean) remains fixed. We estimate the return period and change in intensity of the event in these nonstationary models, in order to compare the climate of the present and the climate of the past, defined respectively by the GMST values of 2023 and of a 1.2° cooler climate representing the preindustrial past (1850-1900, based on the Global Warming Index). 95% confidence intervals are estimated for all quantities by a nonparametric bootstrapping procedure. Typically, results from observations and models that pass the validation tests would be synthesised into a single attribution statement combining the observational and model results; however, as discussed in the next section, we are unable to do so in this case.

3 Observational analysis

Over most of equatorial Africa, especially in the central regions, availability and access to precipitation gauge data is becoming increasingly scarce, resulting in almost complete reliance on satellite and reanalysis products for climate assessments (Awange et al., 2015; Tarek et al. 2021). What is noteworthy is that these products are strongly dependent on gauge data (e.g., Dinku et al., 2018) and passive microwave data (Sun et al., 2018). A result of this is that the various satellite and reanalysis products give extremely diverse estimates in regions where gauge data are particularly scarce, such as the Congo Basin (Nicholson et al., 2019). For instance, huge disparities have been

found in the rainfall distributions from the different observational datasets, for the eastern and western regions of the Congo Basin (Washington et al., 2013). Also, temporal rainfall trends are quite sensitive to temporal changes in gauge network (Harrison et al., 2019). Reanalyses have been found to show the weakest relationship with observed rainfall or with the satellite estimates in this region (Nicholson and Klotter, 2021). As shown in Figures 2 and 3, the available observational products show different intensities and spatial extents of the rainfall in early May 2023. At the same time, the available station data covers only a small part of the region where flooding was experienced. Due to this scarcity of meteorological observations it is very difficult to reliably quantify the magnitude of the event itself, and so to define a return time for the event. Results are therefore presented only for the change in intensity of events in precipitation over these regions, and not for the change in the probability (probability ratio, or PR) that a specific event of this magnitude would occur.

3.1 RX1day over Lake Kivu region

Figure 2 shows the total precipitation on May 2nd - the day on which the heaviest rainfall, and the most severe flooding, were recorded in Rwanda - in the five gridded data products described in Section 2.1, along with the observed precipitation at six stations for which this data was available. The three satellite-based products - TAMSAT, MSWEP and CHIRPS - have fairly similar spatial patterns, with heavy rainfall to the east and northeast of Lake Kivu, where station data confirms that the precipitation was particularly intense; ERA5 registers very low precipitation on this day, while the lower-resolution CPC model has heavy precipitation across far too large a region, including across stations where record levels of rainfall were not recorded.

Figure 4 shows the accumulated daily precipitation from April 1st to May 31st, averaged over the Lake Kivu region enclosed by the grid box outlined in red in Figure 1, in each of the five gridded data products. Only CPC records the precipitation as being particularly high over this region on this date; CHIRPS has moderately high precipitation on the 1st and 3rd, but not on the 2nd; and in all other datasets, rainfall of comparable intensity was recorded in the preceding weeks. This lack of consensus about the amount of rain that actually fell in the region, and when, makes it impossible to define a one-day meteorological event that can defensibly be considered to be related to the severe impacts that were observed, and so makes it impossible to carry out an attribution of the precipitation that can be said to associated with the severe flooding in Rwanda on May 2nd.

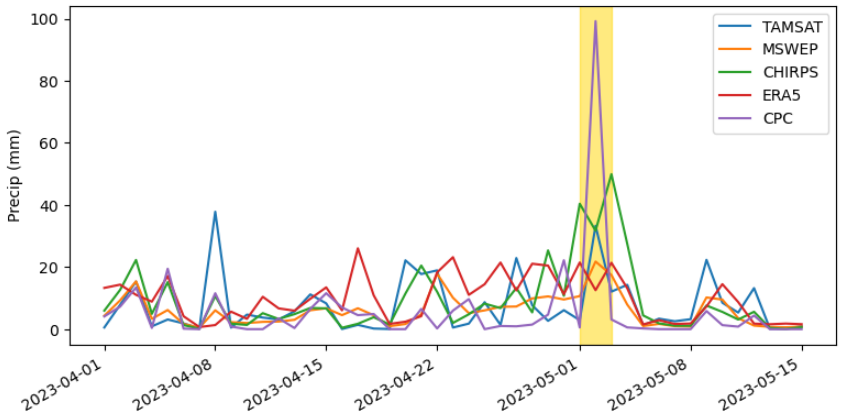

Figure 4: (a) Daily precipitation in five gridded data products over the Lake Kivu region (bounded by a red box in Figure 1). The shaded yellow band marks May 2nd, the period during which the rainfall leading to the heaviest flooding occurred.

3.2 RX5day over DRC/Rwanda region

Figure 3 shows the accumulated precipitation from May 1st-5th in the five gridded data products. Again, the three datasets incorporating satellite data share broadly similar spatial patterns of rainfall over this period, although the intensities differ, with CHIRPS having extremely heavy precipitation over a very large region; in TAMSAT and MSWEP, the precipitation over the DRC/Rwanda region outlined in red was not recorded as particularly heavy over this period compared to precipitation elsewhere in the DRC and Tanzania. ERA5 locates the heaviest rainfall somewhat to the north and south of Lake Kivu, rather than in the area in which the impacts were reported, while CPC has very little topographic structure due to its low resolution. For this reason, neither ERA5 nor CPC are included in further analysis.

Figure 5a shows the 5-daily accumulated precipitation during April and early May over the DRC/Rwanda region. The shaded region highlights May 1st-5th, the days on which the heaviest rainfall and subsequent flooding occurred. Neither TAMSAT nor MSWEP records particularly high 5-day precipitation over the region, while CHIRPS records a peak of around 90mm on average across the region. For this reason, only CHIRPS is used in the subsequent trend fitting analysis. In general, CHIRPS agrees well with the station data provided by MeteoRwanda (see Figure S1 in the supplementary material), and in the two stations where data was available for May 2023 (Gisenyi Aero and Rubengera Met), the RX5day values for 2023 are relatively similar to those in the closest grid cell in CHIRPS. However, we note that MSWEP records heavy precipitation over a substantially larger area than any other dataset in Figure 3, and in the absence of station data across much of the region, we have no way of knowing how accurately this reflects the actual rainfall.

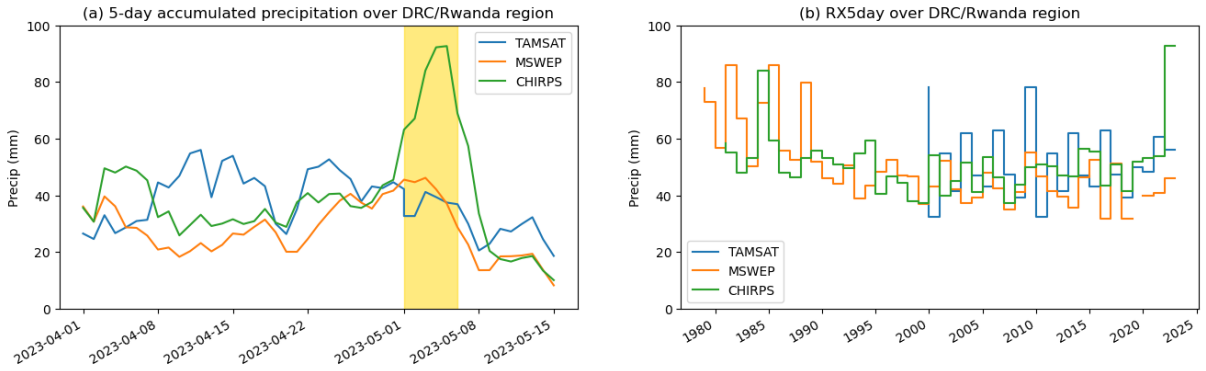

Figure 5: (a) 5-day accumulated precipitation from April 1st-May 15th and (b) MAM maximum of 5-day accumulated precipitation (RX5day) over the DRC/Rwanda region, in the three gridded data products for which the spatial pattern of precipitation was found to be reasonable. The shaded yellow band in (a) marks May 1st-5th, the period during which the rainfall leading to the heaviest flooding occurred.

Figure 6 shows the results of the trend fitting methods described in Philip et al. (2020) applied to the maximum 5-day accumulated rainfall in the MAM season over the DRC/Rwanda region in CHIRPS. Figure 6a shows a slight drying trend in RX5day as a function of GMST, although this is not statistically significant: the change in intensity of the event is estimated at -8.9% (uncertainty: -30% to +18%). However, the GEV distribution is a poor fit to the data (panel b), with several of the observed values falling outside of the 95% confidence interval in the present climate. Returning to panel a, we

note that with the exception of two points, all of the values lie close to the black line that marks the centre of the distribution: these two points are the 5-day maxima in 1985, with an effective return period of 89 years (uncertainty: 22-892 years); and 2023, with an estimated return period of 385 years (uncertainty: 48-3,500,000 years). Experiments with other distributions failed to find a model that provided a good fit to all observations, while removing the two points from the data resulted in a much improved GEV fit (not shown), suggesting that these two data points may be produced by a different process than the one generating the remainder of the points: whether this difference is in the meteorological processes, or in the way the gridded data product is produced, is not known. Due to the high uncertainty on the event magnitude and the return period in this case, we do not present results below for the change in the probability of this particular event occurring, but only consider the expected change in intensity of a hypothetical one-in-400-year event.

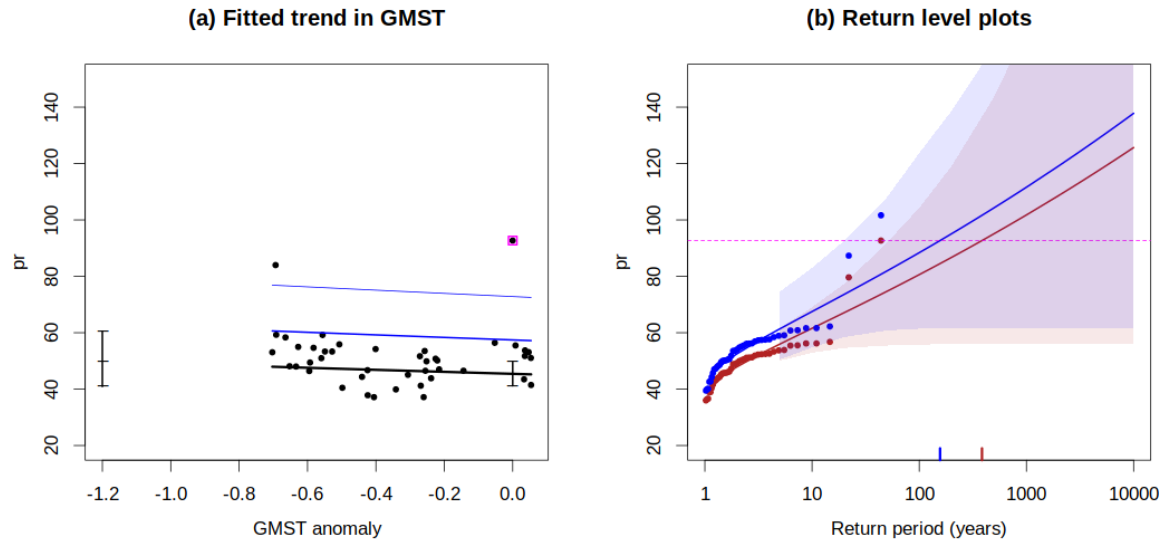

Figure 6: Trend and return level plots for nonstationary GEV fitted to the CHIRPS RX5day time series shown in Figure 5b, with constant dispersion parameter, and location parameter scaled proportional to observed GMST. (a) Observed MAM Rx5day as a function of the smoothed GMST. The black line denotes the time-varying location parameter; the blue lines above indicate 6-year and 40-year effective return levels. The vertical lines show the 95% confidence interval for the location parameter for the 2023 climate and a 1.2ºC cooler climate. The 2023 observation is highlighted in magenta. (b) Return level plots for the climate of 2023 (red) and a climate with GMST 1.2 ºC cooler (blue). The plot shows the goodness of fit of the statistical model (smooth lines) to the data, denoted by points showing the expected return periods against the observed return levels. The shaded areas indicate a 95% confidence interval obtained by a 1000-sample nonparametric bootstrap. The magenta line shows the magnitude of the 2023 event, and the red and blue ticks at the x-axis indicate the return period of the event in the 2023 and 1.2º cooler climates, respectively.

3.3 MAM precipitation over DRC/Rwanda region

The time series of MAM accumulated precipitation over the DRC/Rwanda region is shown in Figure 7. There is little agreement between the three satellite-based data products about which years had particularly wet rainy seasons. Of these three data sets, TAMSAT is only available from 2000 onwards, so cannot be used in the subsequent trend analysis; MSWEP shows rather poor agreement with station data in the 1980s even in stations where performance is good thereafter, suggesting that there may be an overestimation bias during this period (Figure S2 in the supplementary material).

Only CHIRPS seems to agree well with the available station data over the whole period (Figure S3). The observational analysis is therefore again carried out only using the CHIRPS data.

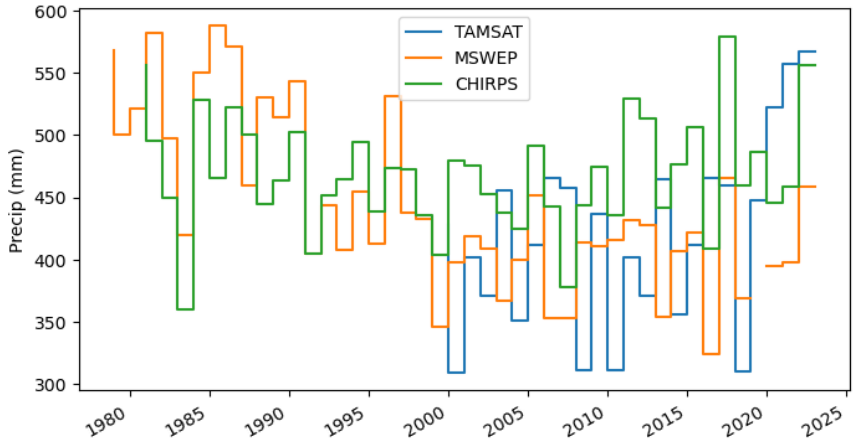

Figure 7: Accumulated MAM precipitation over the DRC/Rwanda region, in the three gridded data products for which the spatial pattern of precipitation was found to be reasonable.

Results of the trend fitting analysis are shown in Figure 8. Here, a slight wetting trend is evident (Figure 8a), although again, the uncertainty is very high and the trend is not statistically significant: the increase in expected intensity of the event is estimated at 3.1% (uncertainty: -12% to +22%). Here, the GEV is a much better fit to the observations (Figure 8b), and the 2023 event is less extreme, with a return period of 31 years (uncertainty: 8-1044 years). A return period of 30 years is used in the attribution analysis; again, results are only presented for the change in expected intensity, not for the change in probability of such an event occurring.

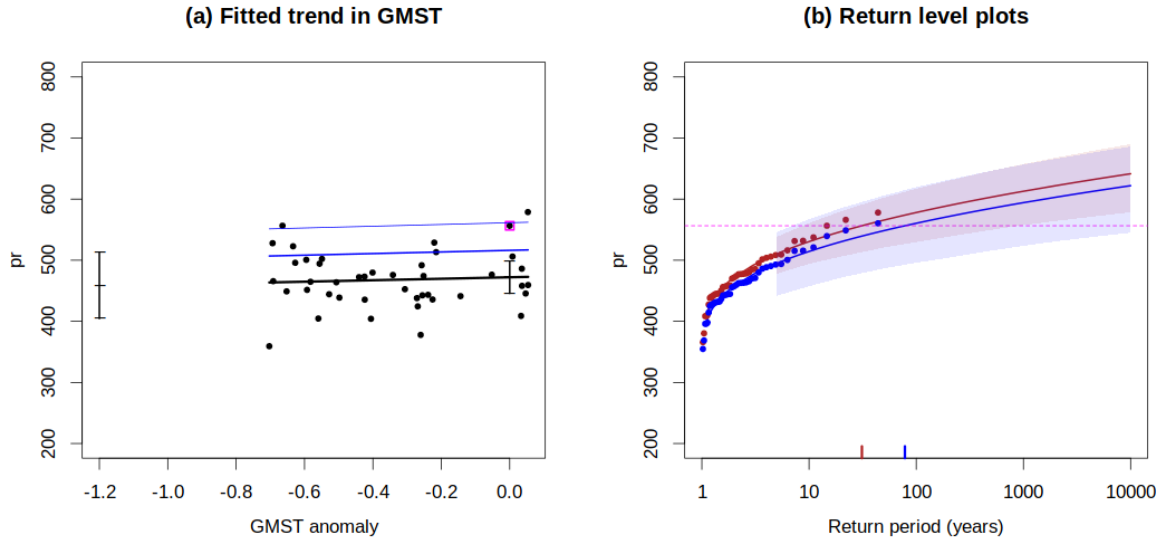

Figure 8: Trend and return level plots for nonstationary Gaussian model fitted to the CHIRPS MAM time series shown in Figure 7, with constant dispersion parameter, and location parameter scaled proportional to observed GMST. Other details are as given in the caption to Figure 6.

4 Model evaluation

Tables 1-2 show the results of the model evaluation for the Rx5day and the season accumulated rainfall in the MAM season, for the DRC/Rwanda region. The evaluation period considered is 1981-2023, the period covered by the CHIRPS data product. If five models or fewer perform well for a particular model setup, we include models that only just pass the evaluation tests for that model setup. The climate models are evaluated against the observations in their ability to capture:

1. Seasonal cycles: For this, we qualitatively compare the seasonal cycle of daily precipitation in the DRC/Rwanda region in the climate model outputs against the cycle computed from CHIRPS. We discard any models that exhibit ill-defined peaks in their seasonal cycles.

2. Spatial patterns: Models that do not match the observations in terms of the large-scale pattern of mean precipitation during March-April-May are excluded.

3. Parameters of the fitted GEV model: We discard the model if the 95% confidence intervals of the shape and dispersion parameters of the fitted GEV do not overlap with those estimated from the gridded observations.

The models are classified as 'good', 'reasonable', or 'bad' based on their performance in each of the three criteria discussed above. If the model is 'good' for all of these criteria, we give it an overall rating of 'good' (green highlight). We rate the model as 'reasonable' or 'bad', if it is rated 'reasonable' or 'bad', respectively, for at least one of the three criteria. These are respectively shown by the yellow and red highlights in the tables below. For the RX5day analysis, three of the nine available CORDEX models met the evaluation criteria, and of the four HighResMIP models, one met the criteria. For MAM, none of the CORDEX models passed the evaluation step, with all of the simulations overestimating the variability of the MAM precipitation relative to its mean level; while only one HighResMIP model passed the evaluation. Also, the regional CORDEX models were reported to agree reasonably well for precipitation projections over Rwanda (Safari et al., 2022). In contrast, most global climate models have been found to misrepresent the variability of East African rainfall, especially the seasonal cycle, by overestimating the OND rains and underestimating the MAM rains (Yang et al., 2016). Most studies have argued that the substantial biases in simulations of the regional climate can be explained by limited representation of the complexity of the interactions between local, regional, and large-scale processes in the region. Notably, the role and effect of the complex East African topography in advection of moisture from the Indian Ocean and Congo Basin (Giannini et al., 2018; Vigaud et al., 2016) and the changing SST trends in tropical Pacific and Indian Oceans (Batté & Déqué, 2011;Tierney et al., 2015). Limited observations to validate and constrain the models also pose a huge challenge (Ayugi et al., 2020; James et al., 2018). There is the potential to use convection-permitting models in attribution analyses in East Africa, however, at the moment no such simulations of sufficient length and ensemble size exist that would allow for the identification of trends in extremes (e.g Finney et al., 2018).

Table 1: Evaluation results for the climate models considered for the attribution analysis of MAM maxima of 5-day accumulated rainfall of 2023 area-averaged over the DRC/Rwanda region. The table contains qualitative assessments of seasonal cycle and spatial pattern of precipitation from the models (good, reasonable, bad) along with estimates for dispersion parameter, shape parameter and event magnitude. The corresponding estimates for observations are shown in blue. Based on overall suitability, the models are classified as good, reasonable and bad, shown by green, yellow and red highlights, respectively.

Model / Observations	**Seasonal cycle**	**Spatial pattern**	**Dispersion**	**Shape parameter**	**Event magnitude (mm)**
CHIRPS			0.139 (0.109 ... 0.179)	-0.077 (-1.1 ... 0.081)	50.2
CORDEX					
HadGEM2-ES_r1_CCLM5-0-15 historical-rcp85 (1)	bad	reasonable	0.207 (0.153 ... 0.255)	-0.35 (-0.78 ... 0.029)	91.128
HadGEM2-ES_r1_RegCM4-7 historical-rcp85 (1)	bad	bad	0.258 (0.173 ... 0.326)	-0.080 (-0.52 ... 0.35)	118.991
HadGEM2-ES_r1_REMO2015 historical-rcp85 (1)	good	reasonable	0.185 (0.139 ... 0.224)	-0.014 (-0.27 ... 0.24)	97.115
MPI-ESM-LR_r1_CCLM5-0-15 historical-rcp85 (1)	reasonable	reasonable	0.211 (0.157 ... 0.307)	-0.36 (-1.1 ... -0.14)	97.612
MPI-ESM-LR_r1_REMO2015 historical-rcp85 (1)	good	reasonable	0.186 (0.141 ... 0.219)	-0.12 (-0.42 ... 0.17)	88.173
MPI-ESM-MR_r1_RegCM4-7 historical-rcp85 (1)	good	bad	0.208 (0.124 ... 0.263)	-0.33 (-1.1 ... 0.096)	108.693
NorESM1-M_r1_CCLM5-0-15 historical-rcp85 (1)	bad	reasonable	0.266 (0.191 ... 0.369)	-0.22 (-1.0 ... 0.32)	102.319
NorESM1-M_r1_RegCM4-7 historical-rcp85 (1)	bad	bad	0.252 (0.194 ... 0.301)	-0.27 (-0.61 ... 0.012)	108.678
NorESM1-M_r1_REMO2015 historical-rcp85 (1)	reasonable	reasonable	0.192 (0.146 ... 0.230)	-0.068 (-0.53 ... 0.32)	89.645
HighResMIP					
HadGEM3-GC31-MM historical (1)	bad	reasonable	0.146 (-0.444 ... -0.0140)	-0.25 (-0.44 ... -0.014)	96
MPI-ESM1-2-HR historical ()	reasonable	reasonable	0.115 (0.0710 ... 0.139)	-0.14 (-0.29 ... 0.13)	77
CMCC-CM2-HR4 historical ()	reasonable	bad	0.135 (0.0900 ... 0.164)	-0.14 (-0.36 ... 0.072)	136
CNRM-CM6-1-HR historical ()	reasonable	reasonable	0.223 (0.161 ... 0.267)	-0.35 (-0.60 ... -0.14)	100

Table 2: Evaluation results for the climate models considered for the attribution analysis of MAM season accumulated rainfall of 2023 area-averaged over the DRC/Rwanda region. The table contains

qualitative assessments of seasonal cycle and spatial pattern of precipitation from the models (good, reasonable, bad) along with estimates for dispersion parameter, shape parameter and event magnitude. The corresponding estimates for observations are shown in blue. Based on overall suitability, the models are classified as good, reasonable and bad, shown by green, yellow and red highlights, respectively.

Model / Observations	**Seasonal cycle**	**Spatial pattern**	**Dispersion**	**Event magnitude (mm)**
CHIRPS			0.0931 (0.0678 ... 0.109)	499.9
CORDEX				
HadGEM2-ES_r1_CCLM5-0-15 historical-rcp85 (1)	bad	reasonable	0.149 (0.114 ... 0.178)	461.853
HadGEM2-ES_r1_RegCM4-7 historical-rcp85 (1)	bad	bad	0.237 (0.182 ... 0.276)	413.931
HadGEM2-ES_r1_REMO2015 historical-rcp85 (1)	good	reasonable	0.145 (0.118 ... 0.166)	444.472
MPI-ESM-LR_r1_CCLM5-0-15 historical-rcp85 (1)	reasonable	reasonable	0.174 (0.116 ... 0.224)	575.357
MPI-ESM-LR_r1_REMO2015 historical-rcp85 (1)	good	reasonable	0.154 (0.117 ... 0.183)	402.995
MPI-ESM-MR_r1_RegCM4-7 historical-rcp85 (1)	good	bad	0.171 (0.132 ... 0.200)	606.760
NorESM1-M_r1_CCLM5-0-15 historical-rcp85 (1)	bad	reasonable	0.223 (0.181 ... 0.254)	465.202
NorESM1-M_r1_RegCM4-7 historical-rcp85 (1)	bad	bad	0.236 (0.190 ... 0.270)	465.158
NorESM1-M_r1_REMO2015 historical-rcp85 (1)	reasonable	reasonable	0.178 (0.140 ... 0.208)	378.969
HighResMIP				
HadGEM3-GC31-MM historical (1)	bad	reasonable	0.130 (0.102 ... 0.156)	636.93
MPI-ESM1-2-HR historical ()	reasonable	reasonable	0.106 (0.0850 ... 0.121)	624.85
CMCC-CM2-HR4 historical ()	reasonable	bad	0.247 (0.192 ... 0.281)	632.06
CNRM-CM6-1-HR historical ()	reasonable	reasonable	0.167 (0.116 ... 0.205)	825.64

5 Multi-method multi-model attribution

Tables 3-4 show the probability ratios and change in intensity for all climate models analysed in the study and also include the values calculated from the fits with observations. However, as discussed in

Section 3, it is difficult to arrive at a reliable event definition due to the lack of consensus between the different observed datasets; therefore, we refrain from inferring conclusions based on PR. The change in intensity is not sensitive to the return period and is suggestive of the effect of climate change, but because the model evaluation is limited by the quality of the observations, it is difficult to synthesise the results.

Table 3: Probability ratio and change in intensity estimates from all the climate models analysed in the study, for MAM maxima of RX5day rainfall for the DRC/Rwanda region.

Model / Observations	a. Past vs. present		b. Present vs. future	
	Probability ratio PR [-]	Change in intensity ΔI [%]	Probability ratio PR [-]	Change in intensity ΔI [%]
CHIRPS	0.41 (0.00012 ... 4.5)	-8.8 (-30 ... 18)		
HadGEM2-ES_r1_CCLM5-0-15 historical-rcp85 (1)	∞ (0.38 ... ∞)	11 (-2.9 ... 25)	1.8 (1.2 ... 27)	7.7 (2.8 ... 12)
HadGEM2-ES_r1_RegCM4-7 historical-rcp85 (1)	17 (0.88 ... ∞)	14 (-10 ... 45)	3.3 (1.0 ... ∞)	5.7 (0.0039 ... 12)
HadGEM2-ES_r1_REMO2015 historical-rcp85 (1)	2.1 (0.28 ... ∞)	5.2 (-5.3 ... 22)	1.4 (0.84 ... 1.0e+2)	3.6 (-2.4 ... 12)
MPI-ESM-LR_r1_CCLM5-0-15 historical-rcp85 (1)	0.36 (0.0 ... ∞)	-2.0 (-13 ... 9.0)	1.4 (0.11 ... 2.0e+4)	2.2 (-3.5 ... 7.2)
MPI-ESM-LR_r1_REMO2015 historical-rcp85 (1)	0.40 (0.0 ... 43)	-4.1 (-19 ... 18)	0.66 (0.000087 ... 1.9)	-2.3 (-7.7 ... 3.9)
MPI-ESM-MR_r1_RegCM4-7 historical-rcp85 (1)	11 (0.0 ... ∞)	3.2 (-14 ... 32)	3.5 (0.46 ... ∞)	4.1 (-2.0 ... 9.2)
NorESM1-M_r1_CCLM5-0-15 historical-rcp85 (1)	13 (0.0 ... ∞)	6.7 (-11 ... 31)	1.5 (0.25 ... 1.0e+2)	2.3 (-4.9 ... 8.8)
NorESM1-M_r1_RegCM4-7 historical-rcp85 (1)	1.1 (0.0 ... ∞)	0.20 (-24 ... 27)	0.78 (0.0 ... ∞)	-0.74 (-7.9 ... 5.7)
NorESM1-M_r1_REMO2015 historical-rcp85 (1)	1.5 (0.0 ... ∞)	2.5 (-21 ... 31)	2.3 (1.1 ... 28)	6.8 (0.85 ... 13)
HadGEM3-GC31-MM historical (1)	2.4 (0.032 ... ∞)	2.6 (-9.3 ... 16)	<not evaluated>	<not evaluated>
MPI-ESM1-2-HR historical ()	0.32 (0.22 ... 2.0)	-4.1 (-13 ... 6.9)	<not evaluated>	<not evaluated>
CMCC-CM2-HR4 historical ()	72 (0.19 ... ∞)	9.6 (-4.9 ... 25)	<not evaluated>	<not evaluated>
CNRM-CM6-1-HR historical ()	0.036 (0.00038 ... ∞)	-15 (-27 ... 0.56)	<not evaluated>	<not evaluated>

Table 4: Probability ratio and change in intensity estimates from all the climate models analysed in the study, for MAM seasonal accumulated rainfall for the DRC/Rwanda region.

Model / Observations	a. Past vs. present		b. Present vs. future	
	Probability ratio PR [-]	Change in intensity ΔI [%]	Probability ratio PR [-]	Change in intensity ΔI [%]
CHIRPS	2.5 (0.014 ... 2.3e+3)	3.1 (-12 ... 22)		

HadGEM2-ES_r1_CCLM5-0-15 historical-rcp85 (1)	6.6 (0.50 ... 73)	9.2 (-2.8 ... 22)	2.1 (1.2 ... 3.3)	4.4 (1.1 ... 7.6)
HadGEM2-ES_r1_RegCM4-7 historical-rcp85 (1)	1.3 (0.039 ... 10)	2.1 (-14 ... 19)	0.84 (0.30 ... 1.7)	-1.1 (-6.0 ... 3.5)
HadGEM2-ES_r1_REMO2015 historical-rcp85 (1)	3.6 (0.32 ... 29)	5.8 (-3.7 ... 16)	1.2 (0.55 ... 2.2)	0.92 (-2.4 ... 3.7)
MPI-ESM-LR_r1_CCLM5-0-15 historical-rcp85 (1)	6.1 (0.78 ... 56)	9.7 (-1.1 ... 23)	2.0 (1.0 ... 4.1)	4.0 (0.25 ... 7.7)
MPI-ESM-LR_r1_REMO2015 historical-rcp85 (1)	0.15 (0.021 ... 0.88)	-13 (-22 ... -1.1)	0.39 (0.11 ... 0.82)	-5.1 (-9.5 ... -1.1)
MPI-ESM-MR_r1_RegCM4-7 historical-rcp85 (1)	0.26 (0.012 ... 2.2)	-9.3 (-24 ... 5.7)	0.40 (0.13 ... 0.87)	-5.1 (-10 ... -0.88)
NorESM1-M_r1_CCLM5-0-15 historical-rcp85 (1)	5.1 (0.40 ... 63)	9.6 (-4.4 ... 26)	2.0 (0.94 ... 3.2)	5.6 (-0.37 ... 10)
NorESM1-M_r1_RegCM4-7 historical-rcp85 (1)	0.18 (0.0067 ... 1.7)	-15 (-33 ... 5.8)	0.49 (0.075 ... 1.2)	-5.7 (-15 ... 2.2)
NorESM1-M_r1_REMO2015 historical-rcp85 (1)	0.63 (0.035 ... 6.3)	-2.9 (-19 ... 11)	0.79 (0.20 ... 1.6)	-1.6 (-8.4 ... 3.8)
HadGEM3-GC31-MM historical (1)	0.23 (0.029 ... 1.1)	-8.7 (-18 ... 0.66)	<not evaluated>	<not evaluated>
MPI-ESM1-2-HR historical ()	0.71 (0.060 ... 7.3)	-1.4 (-10 ... 8.0)	<not evaluated>	<not evaluated>
CMCC-CM2-HR4 historical ()	6.6 (0.50 ... 73)	9.2 (-2.8 ... 22)	<not evaluated>	<not evaluated>
CNRM-CM6-1-HR historical ()	1.3 (0.039 ... 10)	2.1 (-14 ... 19)	<not evaluated>	<not evaluated>

6 Hazard synthesis

As described above, current weather observations in the region are sparse, making it difficult to identify the exact dates and spatial extent of the heavy rainfall that caused the flooding and landslides. While the CHIRPS dataset captures the RX5day event in the available station data, this does not hold for the other two event definitions. Furthermore, even for RX5day the estimated return time is highly uncertain due to the GEV being a poor fit to the data, and without station data available for the whole region there is no way to corroborate or refute any estimates. We thus cannot evaluate the influence of anthropogenic climate change on the likelihood of these events occurring by calculating the probability ratios. However, given that the change in intensity for short-term heavy rainfall is largely independent of the return time of the event in these statistical models, the changes in intensity depicted in Table 3 can serve as an indication of the role of human-induced climate change. However, due to the changes in the gauge network the uncertainty around these trends are quite high. Due to the severe data limitations, and the lack of models passing the evaluation step, we are unable to produce an overarching attribution statement. In line with other research on heavy rainfall in these parts of Africa, the models for the present and future for RX5day show in the majority an increase in the intensity of RX5day rainfall (e.g.,Kimutai et al., 2022) . This is however not the case for all models and uncertainties are generally very large. The results for the MAM seasonal rainfall do not show any clear trends. Given however that models in the region are known to not capture important processes, coupled with the scarcity of observations, these results in no way indicate an absence of a role of climate change, nor that any such change might be small. The data is too poor to draw any conclusions beyond the urgent need to make historic observations available for research, to increase the current observational capacities and to give increased focus to Africa in the development of next

generation climate models.

7 Vulnerability and exposure

Disasters occur when a hazard intersects with the vulnerability and exposure of people, infrastructure, and assets. Vulnerability factors provide an overview of the root causes of the impacts pathways that occur during a disaster and can ranging from pre-existing social vulnerabilities to economic, political and environmental vulnerabilities to hazards (Alcantara-Ayala et al., 2022). This section highlights key aspects of the context in which the severe floods occurred to enable an understanding of why the hydrometeorological event had such significant impacts and offering recommendations for preparedness and adaptation.

The limited data and research about extreme rainfall and flooding in the region significantly hinders the analysis and conclusions which can be drawn about this event. This is as true for both data on the hazard (ie: weather observations), as well as data and region-specific research on the impact, vulnerability, and exposure of people to heavy rainfall, a critical gap that has been highlighted by numerous studies (e.g. Osuteye et al., 2017; Michellier et al., 2020). As such, even the number of deaths and injuries reported by authorities and the press after this event are likely to be different from the actual figures. Therefore, this section highlights the key drivers of vulnerability that are mentioned in the available literature, noting that the dearth of research on the topic in the region limits our ability to be comprehensive.

While floods are a seasonal occurrence in this region, rarely is a single event so deadly. The floods and landslides occurred in an area with high humanitarian needs, degraded land, and underdevelopment. The history of war in the region drives state instability meaning that basic services typically provided by the state such as access to clean water, healthcare, and electricity are underdeveloped or non-existent. Ongoing and protracted conflict, displacement instability, especially in eastern DRC exacerbates the impacts of climate-related shocks and stresses (WFP, n.d.). Some of the affected region is also densely populated, particularly along the lake shores and hillsides, and therefore highly exposed to floods and landslides. The main source of livelihood i.e rain-fed agriculture is also high climate-sensitive.

The DRC ranks at 178 amongst 182 countries in the ND-GAIN Index which measures a country's vulnerability to climate change and other global challenges in combination with its readiness to improve resilience (ND-GAIN, n.d.). Despite its wealth of natural resources, the DRC remains one of the world's poorest countries, with about 73% of the Congolese population living in poverty in 2018 (Sasidharan and Dhillon, 2022). As of 2022, it is estimated that 48.8% of the population in Rwanda is multidimensionally poor[1] (UNDP, 2022). The role of poverty in driving impacts was corroborated by the Rwanda Red Cross through a needs assessment undertaken on 6 May, as findings mentioned that affected homes were generally built with poor construction materials and weak roofing that were no match for the flooding, and people had very limited means of evacuation (IFRC, 2023a). The

[1] The multidimensional poverty index reflects rates of poverty beyond monetary indicators to also consider education and access to basic services and infrastructure such as electricity, water, and sanitation (World Bank, 2022).

COVID-19 pandemic had severe impacts on small-scale businesses in the region, which further reduced household income, rendering this disaster an additional stressor for vulnerable populations (Stoop et al., 2020).

The literature also points to a number of health-related vulnerabilities and impacts. For example, we see that the DRC has the second highest incidence of malaria cases and deaths globally and an infant mortality rate as high as 67/1000 live births (Sasidharan and Dhillon, 2022). Cases of the Ebola virus disease and measles in the DRC continue to be a matter of serious concern. Following the floods, there was a serious concern for the spread of cholera in Rwanda and the DRC as the overcrowding due to a large displaced population and lack of water and sanitation facilities can lead to spread of communicable diseases (IFRC, 2023a). The extreme nature of the event and large death toll is also contributing psychological distress for the affected population (Mason et al., 2010). Additionally, non-communicable diseases (NCDs) in humanitarian settings are less spoken about, but the floods could have massive impacts on people living with NCDs (Schmid and Raju, 2020; Gyawali et al., 2021; Ansbro et al., 2019) especially as the health system in DR Congo has been over-burdened and does not function in many places, which was further worsened during the pandemic (Gorpudolo and Akello, 2021).

7.1 Conflict and displacement

Armed conflict and the instability it brings is a strong driver of disaster vulnerability (Marktanner et al., 2015). It decreases coping capacity, access to support services, increases land exploitation, and destroys infrastructure, social and economic systems which are foundations to resilience and recovery (Schouten et al., 2022; Moodley et al., 2010). For instance, Marktanner et al. (2015) estimate that disaster deaths are 40% higher in places under current armed conflict than those which are not, and the World Bank estimates that the economic cost of conflict in the DRC equates to about 30 years of GDP growth (The World Bank, 2018; Stark et al., 2020).

The DRC and Rwanda have fraught recent histories of conflict of various types, from wars to attacks by armed groups and intercommunal violence across the border and within the countries. The wars of independence of both countries, the Rwandan genocide of 1994, and the first and second Congo Wars were large and widespread events with longlasting impacts. It is estimated that, since 1996, conflict in eastern DRC has led to approximately six million deaths (FRI, 2022). Other flashpoints have arisen over the past two decades in states on the Congo-Rwanda border such as Ituri (Crisis Group, 2020), most often involving ethnic and militant groups with contestations going back to the Congo Wars, and various conflict eruptions particularly around DRC's abundant metals and rare earth minerals with various international interests swarming to the region (Mattysen and Montejano, 2013; Vogel and Raeymaekers, 2016). The region grapples with one of the worst displacement crises driven by people fleeing conflict. UNHCR characterises DRC as the "largest displacement crisis in Africa", with over 5.8 million people internally displaced reported in April 2023 (UNHCR, 2023; OCHA, 2023). In April 2023, the IOM estimated that over 1.5 million displaced people (or 25%) were living in South Kivu itself. The main reasons for this displacement are attacks by armed groups and inter-communal violence (IOM, 2023). These displaced communities are highly vulnerable to all types of shocks, with limited government systems and severely underfunded humanitarian support.

Initial reports highlight that populations displaced due to the disaster "include people with special needs, chronically ill patients, people with disabilities, the elderly, female-headed households,

child-headed households, pregnant women and nursing mothers, etc." (IFRC, 2023b). It must be noted that gender is a factor that exacerbates disaster risk and impacts. In the DRC, during the Ebola outbreak it was observed that gender-based violence increased and this is also a concern highlighted by humanitarian agencies following the current floods and landslides (Stark et al., 2020). It is the presence of "gender-insensitive systems" that amplify disaster risk for women, girls, and other minorities in different forms.

The nature of the transboundary flooding that occurred is also complicated by the current political situation. Political and diplomatic relations between the DRC and Rwanda governments have been on heightened tension in recent months (Acledata, 2023). Cross-border shelling and flight of military aircraft are increasing fears of escalation. Notably, these tensions surround the re-emergence of the M23 rebel group, accused by DRC as being backed by Kigali (Reuters, 2013); a claim denied by the Rwandan government (The East African, 2022).

7.2 Land-use changes

Over the past decades across both the DRC and Rwanda, domestic, regional and global influences have driven significant losses of natural areas that are key to preserving the region's abilities to absorb rainfall, in addition to improving water quality and protecting biodiversity among plants and animals (Depicker et al., 2021). This, in turn, has escalated the risks for flooding and landslides, in part by associated trends in migration which simultaneously increase peoples' exposure to the hazards.

Wetlands have been turned into cultivated lands and built-up areas to increase food and income security in rural South Kivu (Mirenge et al., 2023). The conversion of wetlands depends largely on factors such as annual household income and households' main economic activity along with faulty perceptions of wetlands as wastelands and degraded (Chuma et al., 2022). Today, in North Kivu, a majority depend on agriculture for their livelihood (Philippe et al., 2019).

Another issue in the region is deforestation, notably in South Kivu where most impacts were concentrated in this event. In addition to the need for more farmland, forests are cleared to accommodate the rapid population growth linked to the influx of refugees from neighbouring countries and internal displacement (Villarreal-Rosas et al., 2022; Depicker et al., 2021). Research highlights clear linkages between the emergence of conflicts in the region with an accelerated rate of forest cover loss - a salient example being the Gishwati Forest in northwestern Rwanda, just east of Lake Kivu, as over 80% of which has been converted into pasture land since 1958 when displaced populations started settling in the highlands (Depicker et al., 2021).

The DRC is rich in natural resources. Since the 1990s, international demand for minerals and gold has increased exponentially, leading to more mining activity and associated construction of roads and settlements at the expense of further forest loss (Depicker et al., 2021). The DRC has around 3.5 million metric tonnes of cobalt reserves which represents 74% of the global total. Demand for cobalt, which is a key component in rechargeable batteries used in electric vehicles, has increased rapidly as the world decarbonizes (Fastmarkets, 2023). This places the DRC at the centre of the decarbonization transition, with potential benefits from revenue and foreign investment. But conditions in both the country's artisanal and industrial mines, including allegedly large-scale child labour, have been

described as harsh and dangerous, with workers on "very low pay and subjected to excessive working hours, degrading treatment, violence, discrimination, racism, unsafe working conditions, and a disregard for even basic health provision" (RAID, 2021; Lawson, 2021). The North and South Kivu regions include significant tin reserves as well as gold and coltan. Mining operations can contribute to higher vulnerability to climate hazards by contributing to land degradation, and reducing the availability or quality of water resources for communities (UNEP, 2021; Muimba-Kankolongo et al., 2022). Misaligned trade and security interventions have also fueled inequalities (Koning, 2011).

Depending on the local landscape, deforestation in the Kivu Rift has been known to increase the risk of landslides by a factor of between 10 and 28 (Depicker et al., 2021). Similarly demonstrating the role of forests for the stabilisation of slopes, an analysis by Maki Mateso et al. (2021) showcase that landslides disproportionately occur in areas that have been deforested since the 1960s. Landslide risk is currently twice as high in eastern DRC as in Burundi and Rwanda (Depicker et al., 2021). Still, it has been highlighted that erosion, landslide, and flood risk are all significantly understudied in the region, and contribute to increased vulnerability (IPS, 2023). Aggravating the risk, farming practices are common on old landslides because of the favourable conditions with deeper soils, greater moisture, and higher fertility of the land compared to adjoining flanks (Maki Mateso, 2023). Three-quarters of the surveyed farmers in the Kivu Rift are aware that they are cultivating the soils of old landslides, while 89% of the same assess the risk of landslide reactivation as “high” to “very high” (Maki Mateso, 2023). Unplanned housing in dense urban areas, on unstable slopes and using materials like corrugated iron for roofs both reduces the infiltration of water into the soil and exposes people to dangerous conditions (Sapountzaki et al., 2022). This highlights the precarious livelihood choices with which the populations must contend to meet their basic needs. Further, the populations’ agriculture dependent livelihoods activities will be impacted through loss of crops and livestock. This also has implications for the coming year leading to delays in planting and eventually harvesting crops in an already impoverished region as agriculture activities may not be resumed immediately (IFRC, 2023a; IFRCb, 2023).

7.3 Preparedness, warning, response, and recovery

Preparedness, early warnings, response, and recovery phases of the disaster risk management continuum are key parts of the story of any disaster and essential to highlight here.

Rwanda has a national disaster contingency plan for floods and landslides (developed in 2014 and updated in 2018) which combines a national-level risk analysis and various pieces of scenario planning (MINEMA, 2018). At the time of writing, no after-action reviews have been made public but lessons will be crucial to examine further. The DRC is working on developing a disaster risk reduction policy (GFDRR, 2023) and the DR Congo Red Cross has some plans which cover parts of the country (notably, not including Kalehe. The DRC reports that it used an existing contingency plan from another part of the province in its response to this event) (IFRC, 2023).

While riverine floods are relatively forecastable and can provide adequate lead times for people to act, flash floods and landslides are notoriously more difficult. Both Rwanda and DRC have national hydrometeorological services who have been tracking the development of the unusual season and providing forecasts and warnings. On May 2nd, Météo Rwanda released its May forecast, predicting

“above average rainfall” for the first 10 days and record heavy rainfall for the rest of the month (New Times, 2023). This followed previous outlooks along a similar vein - for example, earlier in April, the US Geological Survey (USGS) and partners had published their outlook for April 2023 which also showed increased streamflow forecasts but an overall average rainy seasons for Rwanda and Burundi with no explicit indication that an abnormal month of May would be expected (USGS, 2023). Global flood forecasting systems such as GloFAS (riverine floods) did indicate an increased risk of heavy floods (1/20 year-flood) in southeastern DRC in late April (GLOFAS). Despite these indications from various weather forecast centres, both the responder and public early warning systems of DRC and Rwanda are sparse - neither country has a standardised system; some forecast information is shared on national news and radios, and certain community early warning systems (both formal and informal) exist primarily on a project basis. Recent efforts are being made to increase the early warning system components in both these countries. Challenges to accessing warning information, however, include the geographic remoteness of certain communities and lack of satellite or phone connection, and even if warnings or information is received, the capacity to interpret the information and to act on it.

The capacity to respond and recover from disasters is relatively limited in both countries - to illustrate, in the Inform Risk Index, the DRC gets a score of 8.1/10 on its lack of coping capacity and Rwanda only relatively better with 5/10 (Inform Risk, 2023). Both national governments hold the authority for disaster response and Red Cross Red Crescent National Societies, as auxiliary to government, are often conducting disaster response and filling in some capacity gaps.

On the 8th of May, the Rwandan government approved the deployment of an emergency response plan that included evacuations and first aid provision (KT Press, 2023). The Rwandan Red Cross submitted an emergency appeal to the International Federation of Red Cross Red Crescent Societies (IFRC)’s Disaster Relief Emergency Fund (DREF) on the 15th of May to cover the affected North, South, and Western provinces. The DR Congo Red Cross did similar with their operations beginning on the 22nd of May to cover the affected Sud Kivu/Kaleh region and included the establishment of an emergency cholera response team (IFRC, 2023). Additionally, for various regions, the region has a significant humanitarian landscape which mobilised during and after the event. During the immediate disaster response phase, agencies such as Médecins Sans Frontières (MSF), UN OCHA, and many NGOS contributed in various ways. For example, MSF’s emergency teams in the South Kivu supported medical equipment provision and medical evacuations (MSF, 2023), UNICEF distributed emergency care kits of different types to affected communities (UNICEF, 2023), and World Food Programme distributed emergency ration; cash transfers were also planned by various agencies (IFRC, 2023).

It is important to note that response in these areas is particularly difficult, not only because the humanitarian needs are very high. Limited road and rail networks, as well as the remoteness of many of the communities, significantly slowed the effectiveness of recovery efforts.

7.4 V&E Conclusions

Rwanda and the DRC are both significantly vulnerable countries to the impacts of climate change. This vulnerability is driven by compound effects of poverty, conflict and political instability, and a range of humanitarian issues notably around health, human rights, and food security. When hazards

hit highly vulnerable people and communities, the impacts are significant, particularly if disaster response and coping capacity are also low.

However, the difficulties of attributing the rainfall to climate change due to data availability mirrors the gaps in data on vulnerability and exposure, notably gaps in country or region specific research on drivers of vulnerability to flooding or socio-economic data. Indeed, the impacts of the event are likely to be underreported, and limited data on vulnerability and exposure limits the depth of analysis that can be done. Despite the gaps, it is clear that protracted conflict, poverty, deforestation, a lack of development and low disaster management and response capacity all contributed to the impacts observed during this event.

In addition, there is an interesting commentary to make about intersecting climate change mitigation and adaptation pathways. The DRC's mineral reserves are critical for global manufacturing as well as the transition to a low carbon economy. However, land and water degradation resulting from deforestation and mining activities, and much of the conflict around these resources, are significant drivers of vulnerability in the region.

As after action review activities begin to take place in the region, and in the acknowledgement that events like this may happen more frequently, it will be essential for those involved to consider how this recovery can contribute to adaptation by decreasing communities' vulnerability and exposure to future events. At the very least, it will be critical to ensure that recovery efforts are not putting these communities at increased risk and creating maladaptation (Magnan et al., 2016).

Data availability

Almost all data will be made available via the Climate Explorer.

Supplementary material

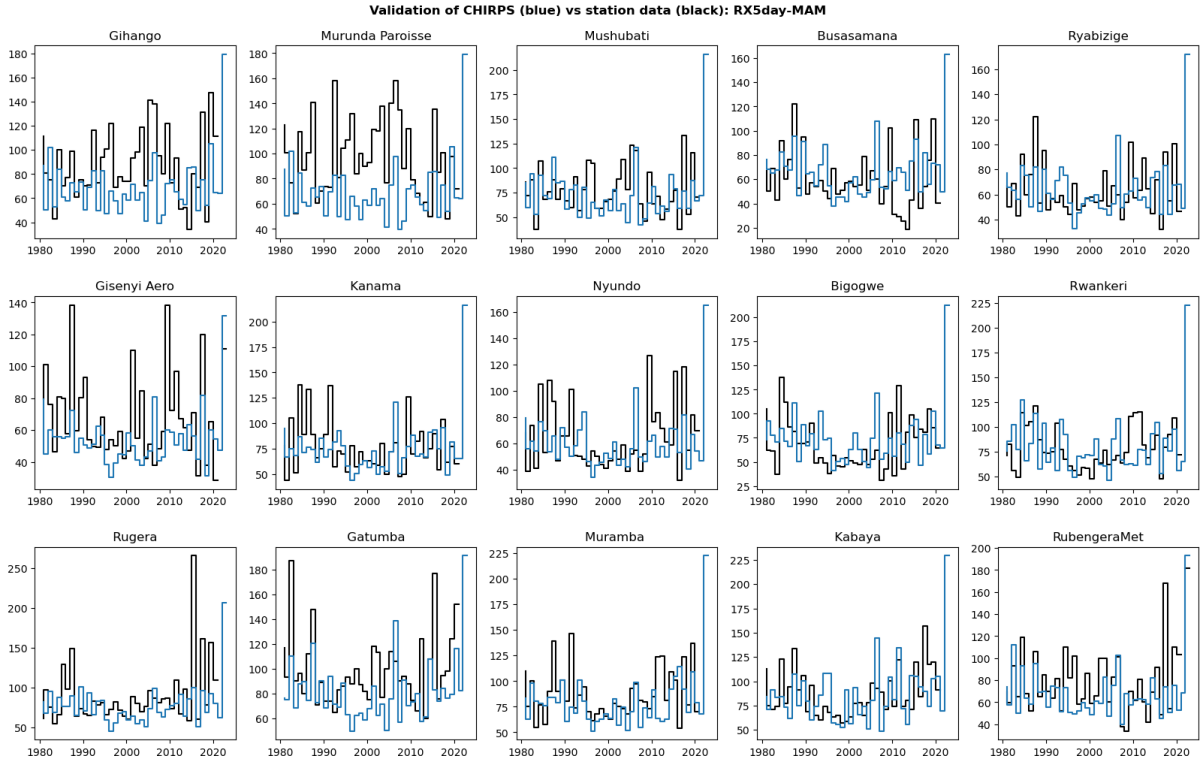

Figure S1: Validation of RX5day in CHIRPS gridded data product against station data. Each panel shows RX5day computed from station data (black), and also in the nearest grid cell to that station (blue lines).

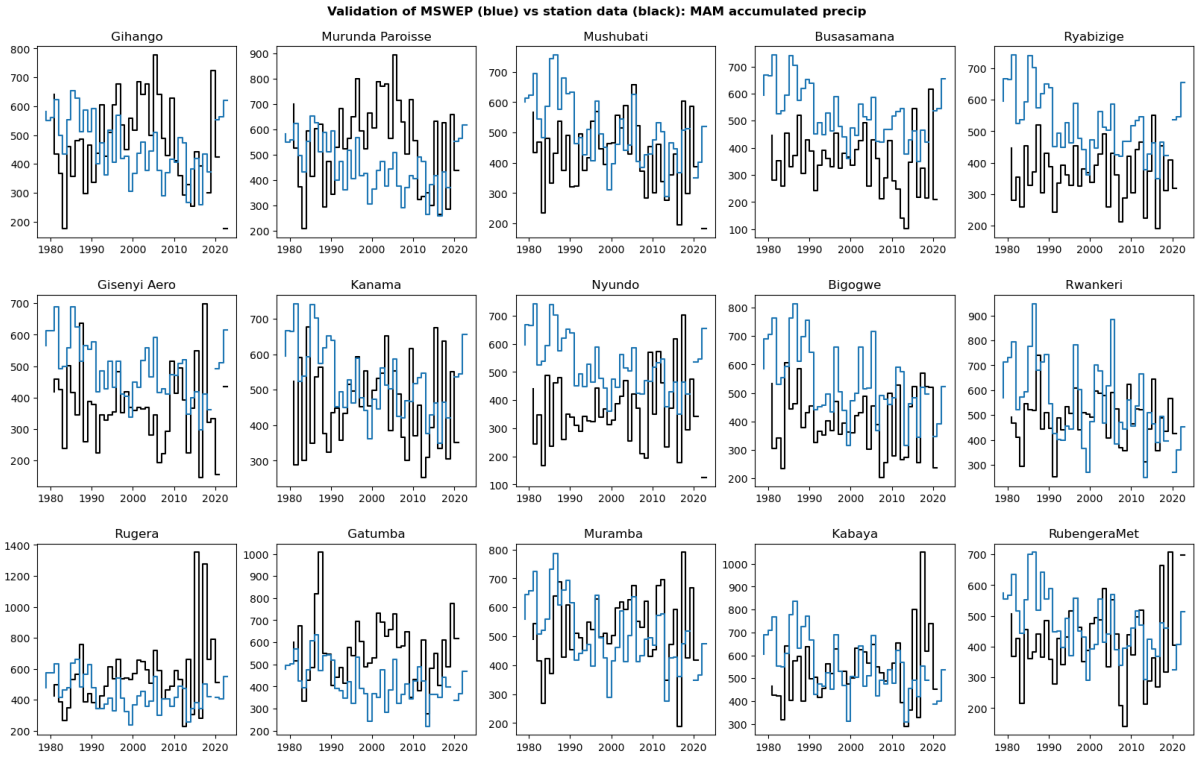

Figure S2: Validation of MAM accumulated precip in MSWEP gridded data product against station data. Each panel shows MAM computed from station data (black), and also in the nearest grid cell to that station (blue lines).

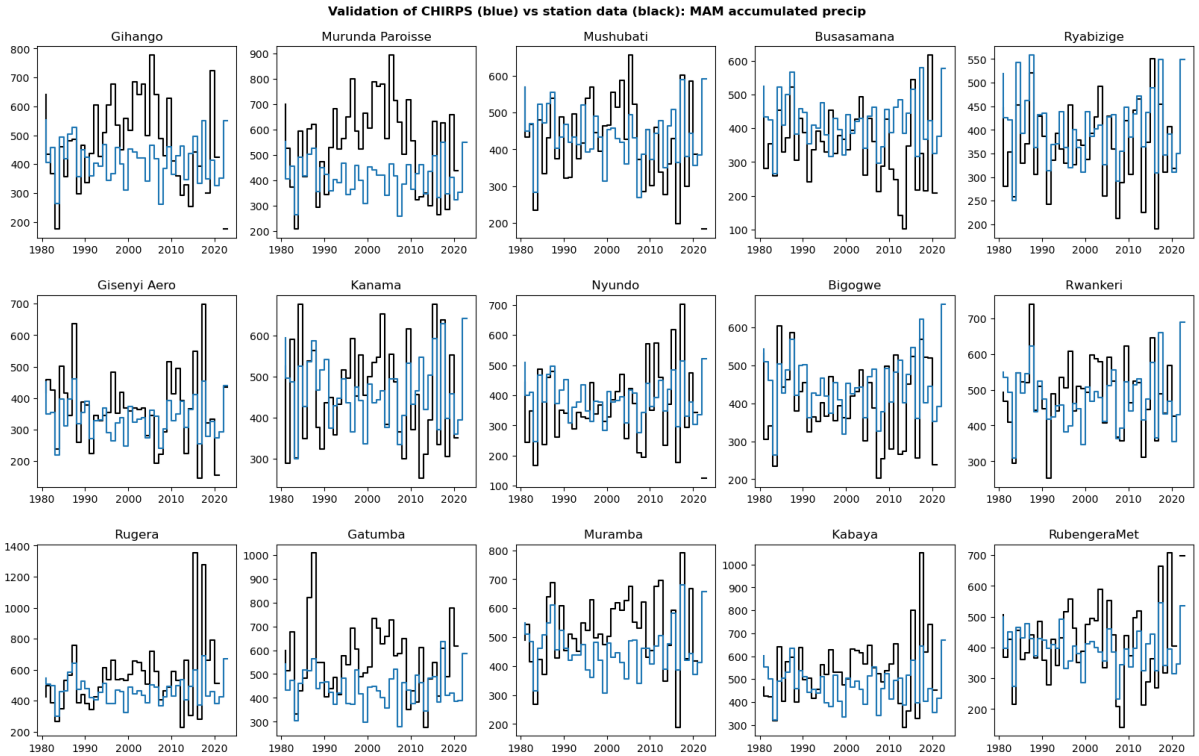

Figure S3: Validation of MAM accumulated precip in CHIRPS gridded data product against station data. Each panel shows MAM computed from station data (black), and also in the nearest grid cell to that station (blue lines).

References

All references are given as hyperlinks in the text.